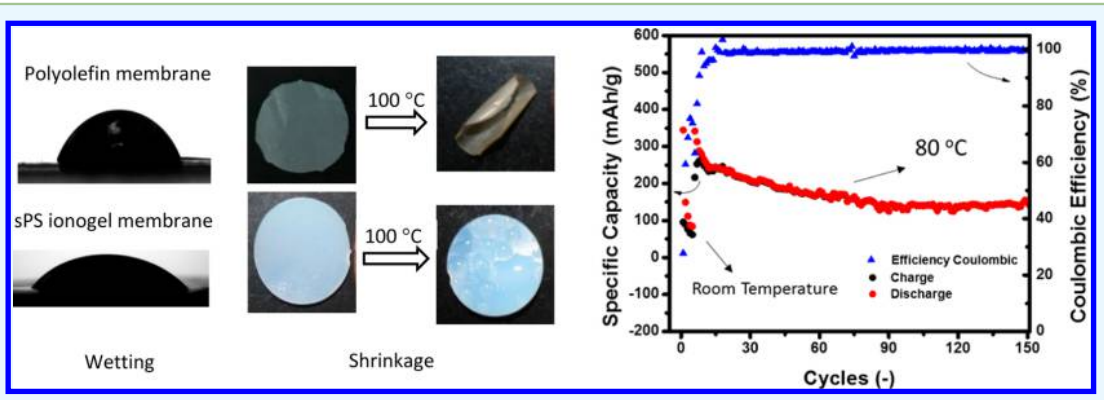


# Syndiotactic Polystyrene-Based Ionogel Membranes for High **Temperature Electrochemical Applications**

Prasad Raut, Wenfeng Liang, Yu-Ming Chen, Yu Zhu, and Sadhan C. Jana\*,

<sup>†</sup>Department of Polymer Engineering and <sup>‡</sup>Department of Polymer Science, University of Akron, Akron, Ohio 44325, United States

Supporting Information



ABSTRACT: This work focuses on ionogel membranes for use in Li-ion batteries fabricated from syndiotactic polystyrene (sPS) gels filled with ionic liquids (ILs). The aim is to increase the operating temperature of Li-ion batteries. Thermal stability and safe operation of Li-ion batteries are two key attributes for their success in hybrid vehicles and other high-temperature applications. The volatility of the liquid electrolytes in current lithium-ion battery technology causes thermal runaway leading to fire, explosion, and swelling of the cell. The approach followed in this work combines the thermal stability and ruggedness of sPS and the extremely low volatility of ILs. The performances of lithium metal/graphite half-cells fabricated with ionogel membranes and those with Celgard-3501 membranes are evaluated at both room temperature and at elevated temperatures of 100 °C. Our data show that the cells with ionogel membranes can be operated continuously at 100 °C without failure. In addition, better charge-discharge capacity is obtained due to high ionic conductivity and high electrolyte retention both derived from high porosity of sPS gels and better wetting of sPS by the ILs.

KEYWORDS: ionogels, Li-ion battery, high-temperature batteries, battery safety, syndiotactic polystyrene, ionic liquids

#### INTRODUCTION

A new generation of high-temperature materials for energy storage applications is the need of time owing to the rise of usage of high-power electric vehicles, aircraft, and pulsed power systems that require energy storage devices for their functions often at elevated temperatures.<sup>1</sup> Lithium-ion batteries (LIBs) present the most suitable storage technology for electric vehicles (EVs) due to their high energy density and better cycling performance over other battery chemistries.<sup>2</sup> The LIBs for hybrid vehicles and other high-temperature applications, for example, moving while drilling (MWD) installations, require safe and thermally stable operation of cells. Current LIB technologies show thermal stability up to 50 °C; at higher temperatures, LIBs lead to hazards like thermal runaway, gas evolution, and ultimately fire; the primary responsible factors are the volatile liquids used as the electrolytes.<sup>3</sup> The battery packs of hybrid electric vehicles (HEVs) and electric vehicles (EVs) are cooled to ambient temperature to prevent the hazards.<sup>1,4</sup> The most common cooling agent is air, while more effective liquid-based cooling systems are incorporated to keep up with the increasing demand of higher power in cars that use

big battery packs. It is reported that these liquid coolants can be conductive when hot and can, in turn, cause the short circuit of the cells.<sup>5</sup> In this context, a high temperature Li-ion battery (HT-LIB) that is stable and produces higher power density can potentially reduce or even eliminate the energy requirements to cool the battery packs and to allow an overall simplified vehicle cooling system.

Traditionally, the cathode and the anode of the LIBs are highly researched areas, while the electrolytes and separators receive much less attention.<sup>6,7</sup> A major source of hazards in LIBs originates from the use of highly volatile organic liquids as the electrolytes.<sup>7-9</sup> The carbonate-based liquids are often limited to usage temperatures below 50 °C due to their high volatility and flammability that often lead to such risks as fire and explosions. Ethylene carbonate (EC), propylene carbonate (PC), and diethyl carbonate (DEC) are the most commonly used carbonate-type liquids used in LIBs. Incidentally, while

Received: June 25, 2017 Accepted: August 17, 2017 Published: August 17, 2017 preparing this manuscript, the authors came across several news reports related to explosion and thermal runaway incidents involving batteries used in Samsung Galaxy Note 7 mobile phones. Even though only several tens of battery failure cases were recorded, Samsung was forced to initially recall the products and eventually discontinue the production and sale of the hazard-associated products, which resulted in a revenue loss in billions of dollars. <sup>10</sup> The root causes for battery failure were identified as inadequate volume to accommodate the negative electrode and the defects originating from welding.<sup>11</sup> The associated thermal run-away events causing explosion and fire were the products of high volatility of the organic liquids. This work provides an alternative to alleviate the concerns associated with the use of highly volatile liquids and thermal stability of the polyolefin membranes currently used in fabrication of LIBs.

The ionic liquids have the potential to replace the hazardous carbonate-type liquids in LIBs due to their nonvolatile nature, nonflammability, and high ionic conductivity. 12,13 Their properties can be tuned using several combinations of cations and anions. In this regard, pyrrolidinium-based ionic liquid, for example, 1-butyl-1-methylpyrrolidinium bis(trifluoromethylsulfonyl)imide (PYR14TF2N) is suitable for high temperature applications as it is thermally stable up to 300 °C and provides ionic conductivity greater than  $1 \times 10^{-3}$  S/cm.  $^{14-16}$ Pyrrolidinium cations offer broad electrochemical window in comparison to imidazolium cations when combined with the same TF2N anions in the IL molecular structure.<sup>17</sup> The presence of such ILs allows the use of anode materials with low electrode potential such as graphite. In this work, the ILs are introduced in LIBs in the form of ionogels where the meso- and macropores of a polymeric gel substrate with porosity greater than 90% are filled with the ILs. 18,19 The ionogel membrane also serves as the separator of the electrodes. In this context, the aggregation of ILs in the pores of dimensions 10-100 nm is known to change their bulk properties including the ionic conductivity. 20,21

This work specifically addressed fabrication of ionogel membranes using macroporous syndiotactic polystyrene (sPS) thermos-reversible gels. 22,23 A specific IL, PYR14TF2N, was incorporated in the pores of sPS gel membrane using solvent exchange method to obtain sPS-ionogel membranes. For comparison, ionogel membranes were also fabricated by filling the pores of polyolefin-based Celgard-3501 separator membranes using the same IL. We note that commercial polyolefin membrane materials change their structural integrity starting at 80 °C and melt at 135 °C (polyethylene) and 160 °C (polypropylene).<sup>24</sup> Therefore, the use of sPS with much higher crystalline melting temperature (270 °C) and glass transition temperature ( $T_g \approx 105$  °C) is expected to produce desired thermal and dimensional stability of the ionogel membranes. To the best of our knowledge, no other study considered sPS ionogel membranes for enhanced electrochemical performance in energy storage devices. Meador and co-workers<sup>25,26</sup> considered a gel electrolyte membrane system for fabrication of LIBs based on the rod-coil block copolymer of polyimide and poly(ethylene oxide) as the host of ILs in their pores. The IL to polymer ratio by weight in such gel structure was greater than 4.0<sup>26</sup> so as to offer high room temperature electrical conductivity of  $6 \times 10^{-6} - 1.2 \times 10^{-5}$  S/cm. Such electrolyte systems offered dimensional stability, reduced interfacial resistance, and higher cycling stability at 60 °C.<sup>26</sup>

#### MATERIALS AND METHODS

Syndiotactic polystyrene (Mw = 300 000 g/mol, density = 1.05 g/mL) was purchased from Scientific Polymer Products Inc. (Ontario, NY). Tetrahydrofuran (THF) was obtained from Sigma-Aldrich and was used as received. Ionic liquid (IL), 1-n-butyl-methylpyrrolidinium bis (trifluoromethane sulfonyl)imide (PYR14TF2N) was obtained from Iolitec Inc. (Tuscaloosa, AL). Lithium bis (trifluoromethane sulfonyl) imide (LITFSI) was procured from Sigma-Aldrich. All the materials obtained were used as received. Copper current collector was purchased from MTI Corp. (Richmond, CA). Anhydrous 1-methyl-2-pyrrolidinone (NMP, Alfa Aesar, 99%) and round punched lithium metal pieces (Li, MTI Corp.) were used as purchased.

The study involved three sets of materials: sPS aerogel monoliths, sPS aerogel membranes, and sPS ionogel membranes. All morphological characterization was conducted using sPS aerogel monoliths and membranes, while the electrochemical tests were conducted using sPS ionogel membranes. In each case, sPS pellets were completely dissolved in THF at 110 °C in a sealed vial to produce a solution of desired sPS concentration as listed in Table 1. The hot solution was

Table 1. Porosity of sPS Aerogel and % IL Uptake in sPS Ionogel

| sPS concentration in solution $\left(g/mL\right)$ | % porosity (P) | wt % IL<br>loading | weight ratio<br>IL/sPS |
|---|----------------|--------------------|------------------------|
| 0.02  | 98             | 98.1               | 51.6                   |
| 0.04  | 95             | 96                 | 24.0                   |
| 0.06  | 93             | 95.5               | 21.2                   |
| 0.08  | 92             | 95.3               | 20.2                   |
| 0.1   | 90             | 95.3               | 20.2                   |
| 0.12  | 89             | 95                 | 19.0                   |

then cast as films of typical thickness  $\sim 100 \ \mu m$  or poured into a cylindrical mold to obtain a gel monolith. For preparation of sPS aerogel membranes and ionogel membranes, the concentration of sPS in solution was 0.08 g/mL, which facilitated casting of the membrane and produced mechanically robust sPS aerogel and ionogel membranes. The sPS ionogel membranes were obtained as follows. A 1 M solution of the electrolyte LITFSI in ionic liquid PYR14TF2N was prepared separately under argon environment and was used to replace THF in sPS gel by repeating the solvent exchange step three times, each time the specimens were kept in electrolyte solution for 24 h. The complete removal of THF was confirmed by FTIR spectroscopy in transmission mode. The sPS ionogel membranes were not subjected to supercritical drying. All the steps involving handling of LITFSI were carried out under inert argon environment in a glovebox. No swelling of sPS was observed due to contact with the ionic liquid.

The sPS aerogel monolith and the sPS aerogel membrane were obtained by drying the corresponding sPS gel specimens using supercritical CO<sub>2</sub>. For this purpose, gel specimens were loaded in a pressure chamber and exposed to liquid CO<sub>2</sub> for 2 h to exchange THF with liquid CO<sub>2</sub>. This process was repeated four times. Afterward, the pressure chamber was heated to 50 °C, and the pressure was raised to 1100 KPa, which was above the supercritical point of CO<sub>2</sub> (31 °C and 740 KPa), and the gas was vented gradually to obtain dry specimens.

Porosity (P) of supercritically dried film and monolithic specimen was estimated from the values of bulk density  $(\rho_b)$  and skeletal density  $(\rho_{\rm s})$ , using eq 1, while  $\rho_{\rm b}$  was obtained from the mass and volume of the specimens, eq 2:

Porosity 
$$(P) = \frac{\rho_b - \rho_s}{\rho_s}$$
 (1)

$$\rho_{\rm b} = \frac{4m}{\pi D^2 h} \tag{2}$$

In eq 2 m is mass of the sample, and D is the diameter of cylindrical sPS aerogel monoliths of height h. Skeletal density  $(\rho_s)$  was determined using helium pycnometer (AccuPyc II 1340 Series, Micromeritics Instrument Corp GA, USA).

The weight percent of IL in ionogel (percent IL loading) was estimated from gravimetric analysis of the specimens after each stage of the solvent exchange process until THF was completely removed. Each solvent exchange step needed 24 h.

The porous morphology of the membrane materials was observed using scanning electron microscopy (JEOL JSM5310) with operating voltage of 5 kV. For this purpose, membrane specimens were dried using supercritical CO<sub>2</sub> using the procedure presented above. The dried membrane materials were fractured at room temperature and mounted on the aluminum stub using conductive carbon tape. The stubs were later sputter-coated under argon atmosphere using ISA 5400 sputter coater. The degree of filling of the pores in ionogel membranes was studied using environmental SEM.

MacMullin number,  $N_{\rm m}$  was obtained by measuring the conductivity of the electrolyte in membranes, as in eq 3:  $^{24,27}$ 

$$N_{\rm m} = \frac{R_{\rm s}}{R_{\rm e}} \tag{3}$$

In eq 3,

 $R_{\rm s}$  = specific resistivity of the ionogel membrane.

 $R_{\rm e}$  = specific resistivity of the electrolyte.

Specific resistivity (R) was calculated using eq 4 from the values of measured resistance of separator  $(R_e)$  in  $\Omega$ , the electrode area in centimeters squared (A), and the thickness of the membrane in centimeters (1):

$$R = \frac{R_e A}{l} \tag{4}$$

For this purpose, LiTFSI was dissolved in PYR14TFSI to obtain 1 M electrolyte solution. The membranes soaked in electrolyte solution were compressed between two stainless steel plates and the resistance of the membranes was measured using an electrochemical station (CH Instruments, CHI608E). The membrane thickness was measured from optical microscope image of the film cross-section.

Differential scanning calorimetry (DSC, TA Q200, TA Instrument, NewCastle, DE) was used to study the thermal behavior of the materials. The thermal properties, such as melting temperature ( $T_{\rm m}$ ) and glass transition temperature ( $T_{\rm g}$ ), were determined at a ramp rate of 10 °C/min in sealed hermetic pans under N<sub>2</sub> purge flow of 50 mL/min. Thermal stability was investigated using thermogravimetric analysis (TGA Q50 TA Instruments) under nitrogen environment at a heating rate of 10 °C per minute. The temperature at the onset of thermal degradation or the % loss of mass was estimated from the mass versus temperature traces.

To study dimensional stability at high temperature, circular discs of ionogel specimens were heated at 100 °C, and the diameter was noted to obtain diameter shrinkage as per eq 5 from the values of initial diameter  $(D_0)$  and final diameter  $(D_f)$ :

% Shrinkage (%D) = 
$$\frac{(D_0 - D_{\rm f})}{D_0} \times 100$$
 (5)

Rame-Hart model 500 advanced goniometer was used for water contact angle measurements. Static sessile drop technique was used with a 4  $\mu$ L drop of liquid placed on the sample surface, and the images were captured. Five measurements were taken for each specimen. The dried porous specimens were compressed under 30 MPa pressure to remove the pores and to obtain smooth solid discs. The contact angle measurement was carried out using a 1:1 (w/w) mixture of ethylene carbonate and dimethyl carbonate and neat PYR14TF2N at room temperature to compare the wetting characteristics of sPS by the above liquids.

Tensile strength of sPS was measured at room temperature and at 100 °C. For this purpose, supercritically dried sPS aerogel monolith bars were compressed in a compression mold to obtain a film of uniform thickness. The sPS monoliths were used instead of virgin sPS pellets so as to capture the effects of crystalline sPS strands that developed in the gel specimens. The specimens were subjected to a

tensile extension rate of 1 mm/min. The measurements were performed at a fixed temperature under a temperature-controlled environment.

Coin cell fabrication involved the following steps. The electrode slurry was prepared by mixing synthetic graphite powder with carbon black and polyvinylidene fluoride (PVDF) at a ratio of 8:1:1, respectively, with NMP. The slurry was subsequently cast on the copper foil using a doctor blade and then dried overnight in an oven at 100 °C. The as prepared electrode foil was punched into circular discs of 7.93 mm in diameter, using 5/16" punch hole and a mass loading of 0.7-0.9 mg cm<sup>-2</sup>. Coin cells (CR2032, MTI Corp., USA) were assembled using lithium foil as the counter electrode and 1 M LiTFSI solution in PYR14TFSI ionic liquid as the electrolyte and installed by applying pressure of 6.9 MPa with a Hydraulic Crimper (MSK-110, MTI Crop., USA). Coin cell 2032 assembly was chosen based on prior experience and the availability of the assembling unit. Compressive forces on the membranes may vary based on the type of coin cell components. Porous polypropylene (Celgard 3501, Celgard, LLC Corp., USA) and as synthesized sPS membranes were used as the separator. Celgard-3501 membrane specimens were kept in a 1 M solution of the electrolyte, LITFSI, in ionic liquid PYR14TF2N for 8 h at 30 °C to ensure complete wetting by the electrolyte. Electrochemical test was conducted by using an 8 channel battery analyzer (BST-8A, 1 mA, MTI Corp., USA) at room temperature and at high temperature in an isothermal chamber assembled in house. The isothermal chamber was able to sustain a temperature of up to 200 °C. Galvanostatic charge/discharge tests were carried out in the voltage range of 0.01-3.0 V.

Linear sweep voltammetry (LSV) was performed in the following configuration: stainless steel platelmembrane with electrolytellithium foillstainless steel. The voltage scans were performed directly on these half cells. A scan rate of 0.5 mV/s in the range of 0–7 V was used. The data on electrochemical impedance spectroscopy (EIS) were measured by CH Instruments CHI608E, in the frequency range of 100 kHz to 0.1 Hz with a perturbation voltage of 5 mV. The following configuration was used: stainless steel platelmembrane with electrolytelgraphite electrode.

### ■ RESULTS AND DISCUSSION

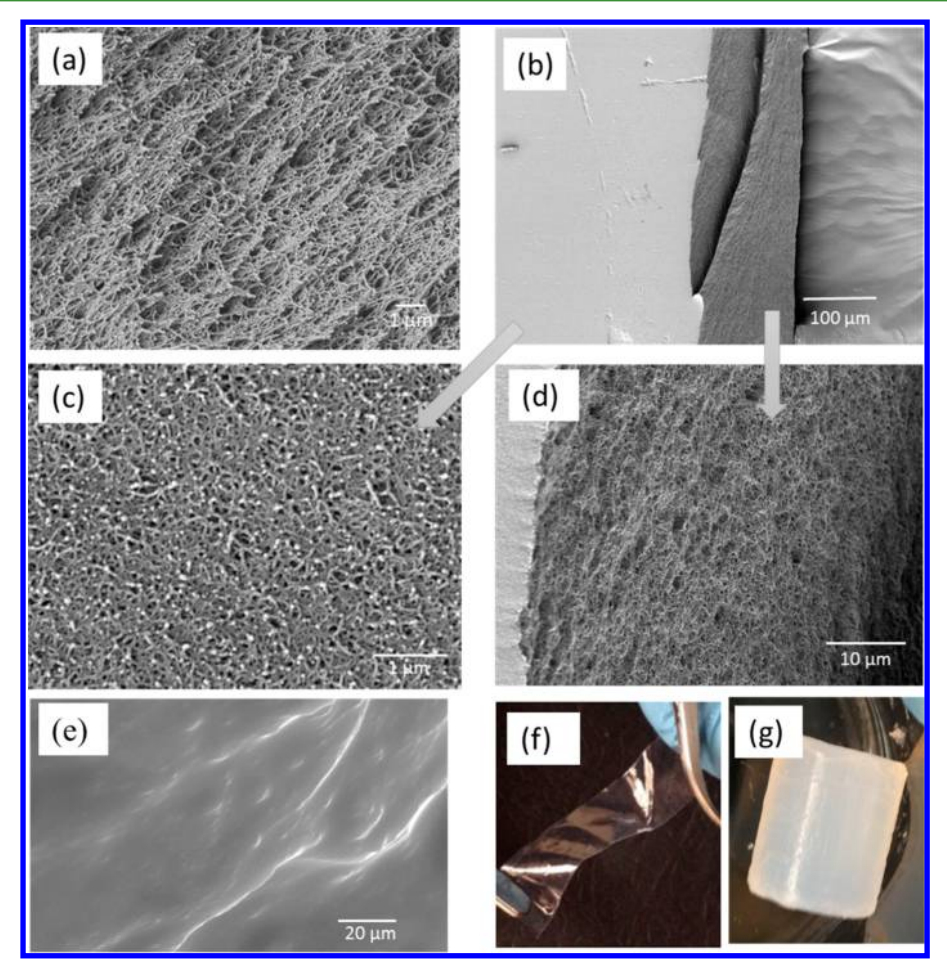
The porosity of sPS aerogel, as listed in Table 1, has two functions. First, the pore volume serves as a reservoir for the electrolytes in the corresponding ionogel membrane. Second, the pores filled with the electrolyte provide channels for unhindered ionic current flow. It is intuitive that porosity listed in Table 1 should reduce with an increase of the polymer concentration in the precursor sPS solution in THF, for example, 98% for 0.02 g/mL versus 89% for 0.12 g/mL. Nevertheless, the porosity values were significantly higher (89–98%) than that of Celgard-3501 membrane (55%), see Table 2.

Table 2. Data on Celgard-3501 Specialty Membranes

| porosity <sup>a</sup>                 | 55%        |
|---------------------------------------|------------|
| thickness <sup>a</sup>                | $25 \mu m$ |
| shrinkage <sup>a</sup> @ 90 °C        | 5%/h       |
| JIS Gurley (sec) <sup>a</sup>         | 200        |
| wt % IL loading for Celgard- $3501^b$ | 62.6       |

<sup>a</sup>Data obtained from product literature, ref 26. <sup>b</sup>Data from measurement in present work.

Accordingly, IL loading in ionogel membranes was significantly higher (95–98 wt %) compared to  $\sim\!63$  wt % for Celgard-3501 membrane as listed in Tables 1 and 2. The weight ratio of IL to polymer varied between 19 and 52. The wt % of IL was obtained from gravimetric analysis data. The lower %IL uptake in Celgard-3501 membrane is a reflection of its lower porosity



**Figure 1.** Scanning electron microscope images (a) fracture surface of sPS aerogel monolith, (b) sPS aerogel membrane, (c) top surface of the membrane, (d) cross-sectional surface of the membrane, (e) cross-section of 1 M LITFSI filled sPS ionogel membrane. Optical microscope images of (f) sPS ionogel membrane and (g) sPS ionogel monolith.

content of 55%. In this context, lower Gurley value and accordingly lower electrical resistance are anticipated for systems with high porosity, <sup>24</sup> for example, in the sPS ionogel considered in this work. Even though the Gurley values were not measured for sPS ionogel membranes, it is apparent from the porosity data that the Gurley value for sPS ionogel membranes would be much less than that of Celgard-3501 membrane.

The scanning electron microscope images of sPS aerogel monolith and corresponding membrane materials are presented in Figure 1a and b, respectively. The enlarged views of top of the membrane and the cross-sectional area of the aerogel membrane are presented, respectively, in Figure 1c and d. It is seen that the top surface of the membrane is porous and should maintain reversible transport of ions between the membrane and the electrode. Figure 2 shows highly elongated pores in the SEM image of Celgard-3501 membrane, whereas the pores evident from the cross-sectional area of the supercritically dried sPS aerogel films as seen in Figure 1d show highly tortuous networks. Such a tortuous pore network is desired to suppress the growth of lithium dendrites. Figure 1e shows the SEM image of cross-section of sPS ionogel membrane containing the electrolyte. This image indicates that the pores were filled by the electrolyte. Figure 1f and g show the images of freestanding transparent sPS ionogel membrane and translucent monolithic of sPS ionogel cylinder filled with 1 M LITFSI in PYR14 TFSI.

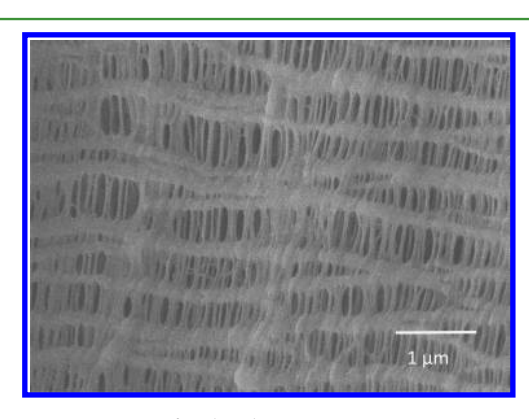
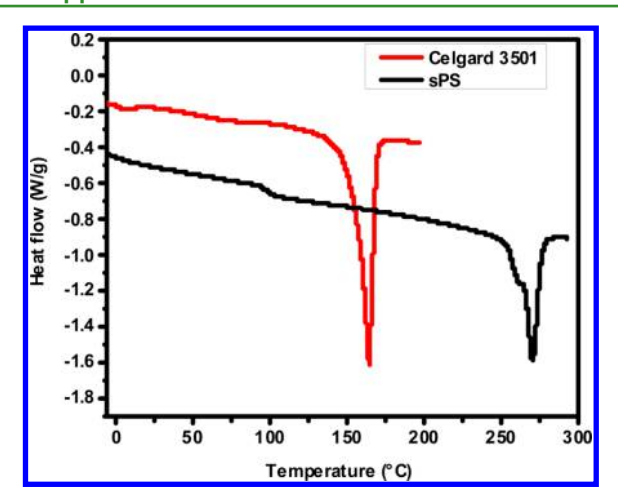
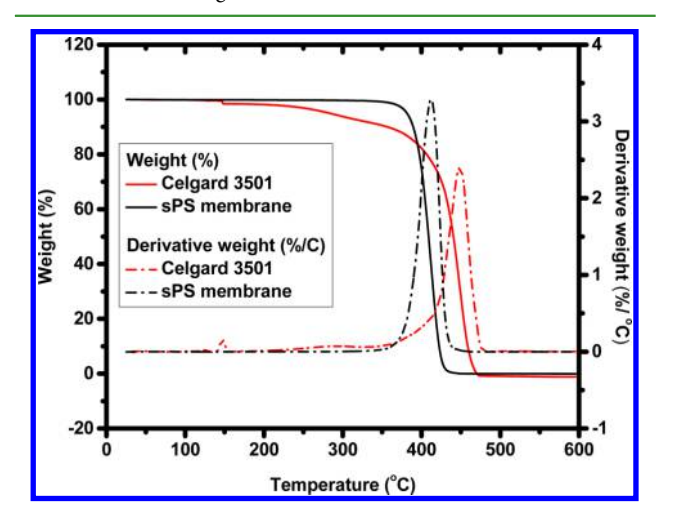


Figure 2. SEM image of Celgard-3501.

Thermal stability of electrolytes is a critical requirement for the safety and stability of LIBs in applications. In this regard, thermal properties of ionogel specimens were investigated using DSC and TGA data. Figure 3 shows the DSC traces of the ionogel and Celgard membranes filled with the electrolyte. It is seen that the polymer in Celgard-3501 membrane melted at around 164 °C, while the sPS shows complete melting at 274 °C. These results indicate that high melting sPS ionogel membranes are more suited for high-temperature applications. Figure 4 shows the TGA traces of the ionogel membrane materials. The weight of the sPS ionogel remained unchanged up to 350 °C, while the Celgard-3501 ionogel showed weight



**Figure 3.** Differential scanning thermograms of ionogel membranes bases on sPS and Celgard-3501.



**Figure 4.** TGA traces of ionogel membranes based on sPS and Celgard-3501 at a scan rate of 10  $^{\circ}$ C/min under nitrogen environment.

loss starting from 150 °C. The dotted lines in Figure 4 represent the DTG curves, that is, derivative of weight loss versus temperature. The structural integrity of the membrane was lost after melting of the polymer and complete degradation peak of the material appeared at ~400 °C in the case of Celgard-3501 ionogel membrane. For sPS ionogel membrane, no peak appeared in DTG curve before the material started its degradation at around 350 °C with a peak in DTG curve at ~450 °C. The data in Figure 4 reinforce much better thermal stability for sPS ionogel membranes compared to Celgard ionogel membrane. The small weight loss observed for Celgard ionogel membrane at temperatures between 100 and 200 °C can be attributed to loss of moisture and quite possibly the coating materials that are used in Celgard materials for promotion of wetting by the liquid electrolytes.

The effect of long-term exposure to high temperature was evaluated by keeping the membrane materials in a convection oven at 100 °C. After 24 h, the Celgard ionogel membranes showed signs of degradation as it turned brown and the specimen diameter reduced by 39% with a loss of 87% IL from the system (Figure 5a,b). The observed shrinkage of Celgard-3501 ionogel membrane was lesser than what was reported for Celgard-3501 membrane as presented in Figure 5b. On the other hand, sPS ionogel did not show signs of degradation after 24 h of exposure (Figure 5c,d). The sPS ionogel membrane experienced 16% IL loss and a reduction of 13% in diameter only in the first 24 h of observation period. These can be attributed to differences in thermal expansion coefficient, for example,  $\sim 6.8 \times 10^{-4} \text{ K}^{-1}$  at 87 °C<sup>28</sup> of IL and  $\sim 2.0 \times 10^{-4} \text{ K}^{-1}$  at 20–100 °C of sPS, <sup>29</sup> and due to transformation of the  $\delta$ form sPS crystal to higher density  $\gamma$ -form crystals caused by thermal annealing. <sup>30</sup> The ionogel membranes did not show any change of IL loading or shrinkage in the next 24 h of exposure to heat at 100 °C (Figure 5e).

Wettability of a separator membrane is an important parameter for battery fabrication and performance. Wettability mainly depends on porosity, surface roughness, viscosity of the liquid electrolyte, and the chemical affinity between the electrolyte and the membrane surface.<sup>31</sup> To investigate

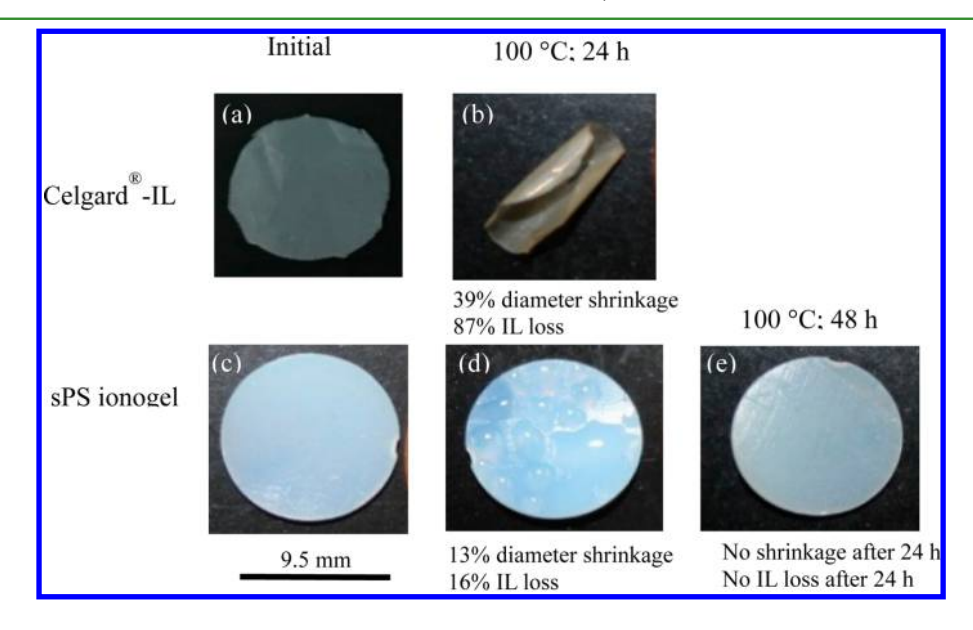


Figure 5. State of ionogel membranes as a function of exposure to heat at 100 °C. Celgard-IL membrane: (a) initial, (b) after 24 h. sPS-IL membrane: (c) initial, (d) after 24 h, and (e) after 48 h.

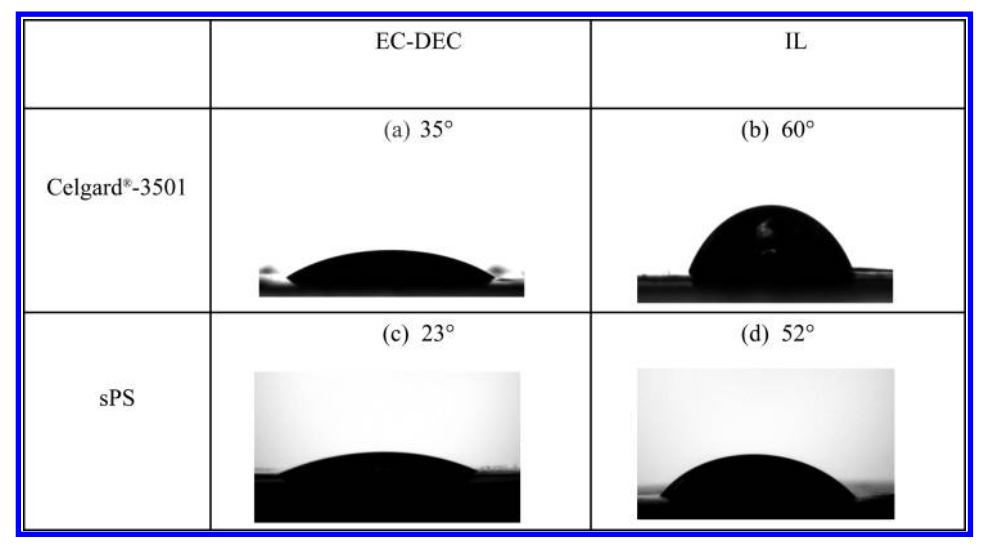


Figure 6. Contact angle of various liquids on membrane materials. (a) EC-DEC on Celgard -3501 membrane, (b) PYR14 TF2N on Celgard-3501 membrane, (c) EC-DEC on sPS membrane, and (d) PYR14 TF2N on sPS membrane.

wettability, contact angle values of the liquid electrolytes were measured on porous surfaces of Celgard-3501 and sPS membranes. For this purpose, a 1:1 by weight mixture of traditional ethylene carbonate (EC) and diethyl carbonate (DEC) liquid and neat PYR14TF2N ionic liquid were used. Figure 6 shows the contact angle values on Celgard-3501 and sPS membranes. It is apparent that both the traditional, that is, mixture of EC and DEC and IL electrolyte show better wettability of sPS surfaces. The lower values of contact angle on sPS membranes represent an excellent wettability of the surface by the corresponding electrolyte.

MacMullin number  $(N_m)$  represents the resistance of porous membranes to ionic conductivity. In this sense, a low MacMullin number is desirable.<sup>24,32</sup> The data in Table 3

Table 3. Membrane Properties of a Commercial Celgard-3501 and sPS Ionogel Membrane at Room Temperature

| sample  | $egin{array}{l} 	ext{MacMullin} \ 	ext{number} \ 	ext{} (N_{	ext{m}}) \end{array}$ | ionic<br>conductivity<br>(S/cm) |
|---|--|---------------------------------|
| Celgard-3501 + 1 M LITFSI in PYR14TF2N                              | 20.5   | $4.88 \times 10^{-5}$           |
| sPS-ionogel (0.08 g/mL concentration in THF + 1 M LITFSI PYR14TF2N) | 1.6  | $6.33 \times 10^{-4}$           |

indicate the ionic conductivity and MacMullin number for sPS ionogel and Celgard-3501 ionogel membranes. The conductivity value for 1 M LITFSI in PYR14TFSI was obtained from literature as  $1 \times 10^{-3}$  S/cm. The resistance of 15 mm diameter membranes soaked with the electrolyte solution was measured. The ionic conductivity of sPS ionogel membrane at room temperature was found to be  $6.33 \times 10^{-4}$  S/cm, whereas the value for 1 M LITFSI soaked into Celgard-3501 membrane was an order of magnitude lower, at  $4.88 \times 10^{-5}$  S/cm. These conductivity values are higher in reference to the room temperature conductivity values, for example,  $6 \times 10^{-6}$ -1  $\times$ 10<sup>-5</sup> S/cm reported by Meador and co-workers, <sup>25,26</sup> and are attributed to much higher IL to polymer weight ratio of 19-52 compared to slightly greater than 4.0 in the work of Meador et al. 25 As seen in Table 3, the value of  $N_{\rm m}$  (1.6) for sPS ionogel membranes is much smaller than that of Celgard-3501 ionogel membrane (20.6). The higher ionic conductivity observed for sPS ionogel membrane can be attributed to its higher porosity

values (see Table 1) and better wettability as observed from the contact angle data listed in Figure 6.

The ionogel membrane materials should be strong enough to withstand the mechanical handling during cell winding and assembly processes. Figure 7 shows the stress versus strain

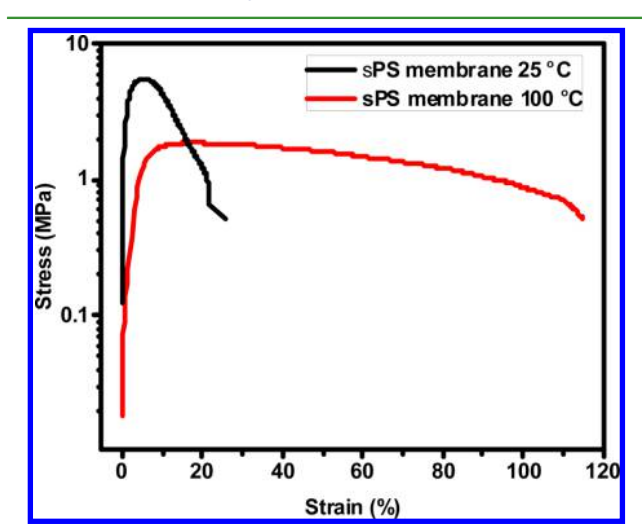


Figure 7. Stress versus strain plot for sPS ionogel membranes at 25 and 100 °C.

diagram for sPS ionogel membrane evaluated at 25 and 100  $^{\circ}$ C. The sPS ionogel membrane shows high Young's modulus of 6 MPa at 25 °C and can withstand mechanical handling during cell fabrication. As is intuitive, the Young's modulus value decreased to 2 MPa at 100 °C, although, this modulus value ensured continuous operation of the cell at 100 °C without yielding and eventual failure. Further strengthening of the membrane will be desired to enable translation of this technology to larger scale battery manufacturing, especially when thinner membranes are desired in the future.

The electrochemical tests were conducted for cells fabricated with ionogel membranes based on both Celgard-3501 and sPS. Electrochemical impedance spectroscopy (EIS) technique was used for analysis of the connection and compatibility between electrodes and membrane. In Figure 8, the Nyquist plots are

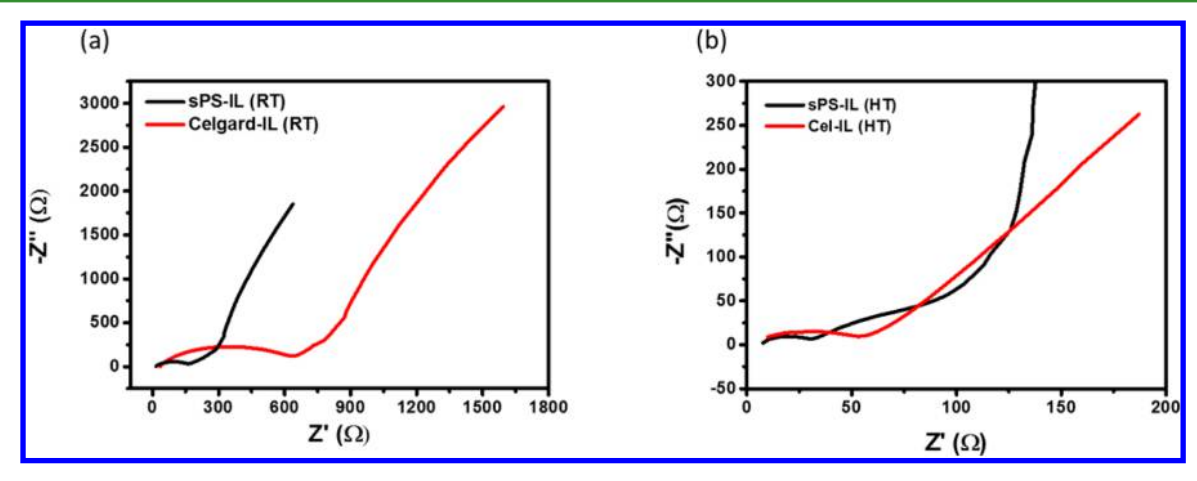


Figure 8. Impedance spectra for sPS ionogel and Celgard-3501 ionogel membranes (a) at 25 °C and (b) 100 °C.

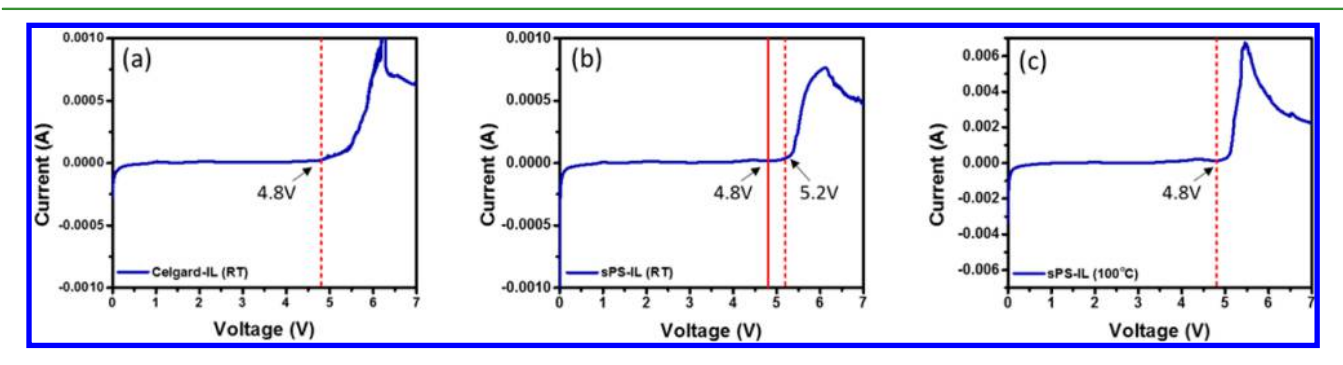


Figure 9. Linear sweep voltammogram for Li-ion battery with (a) Celgard-3501 ionogel membrane at 25  $^{\circ}$ C, (b) sPS ionogel membrane at 25  $^{\circ}$ C, and (c) sPS ionogel membrane at 100  $^{\circ}$ C.

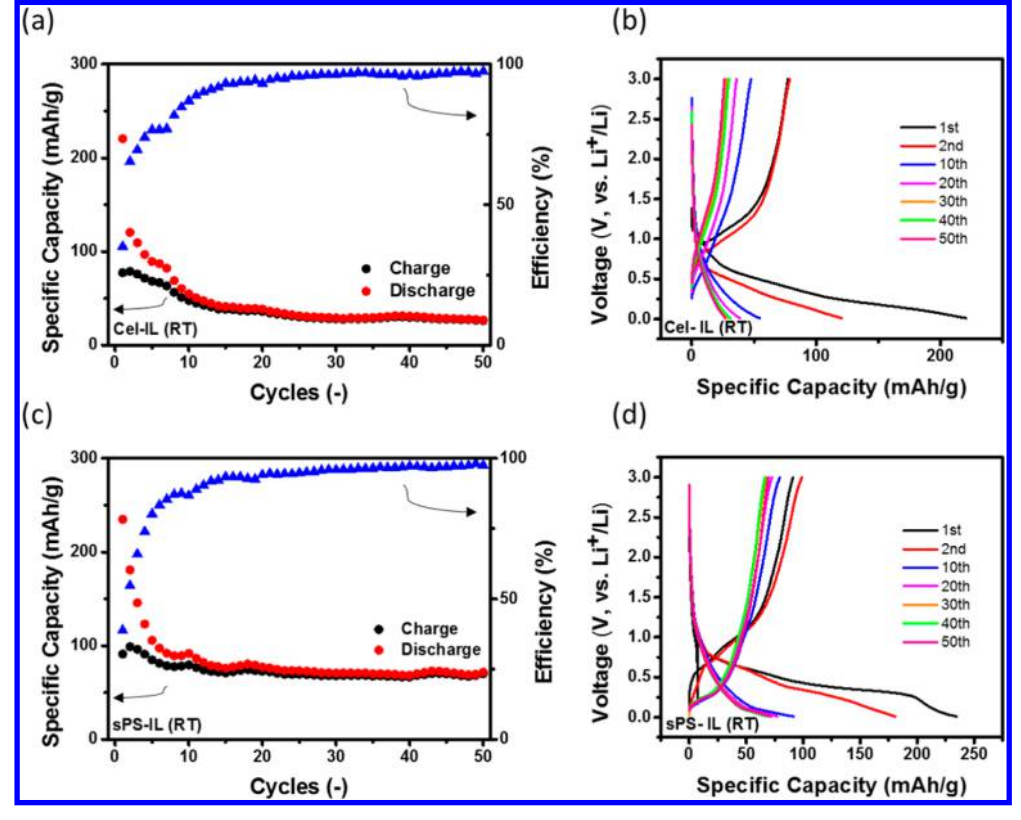


Figure 10. Cycling performance and Coulombic efficiencies of (a) Celgard-IL and (c) sPS-IL at room temperature, and the corresponding charge/discharge profiles (b, d).

**ACS Applied Materials & Interfaces** 

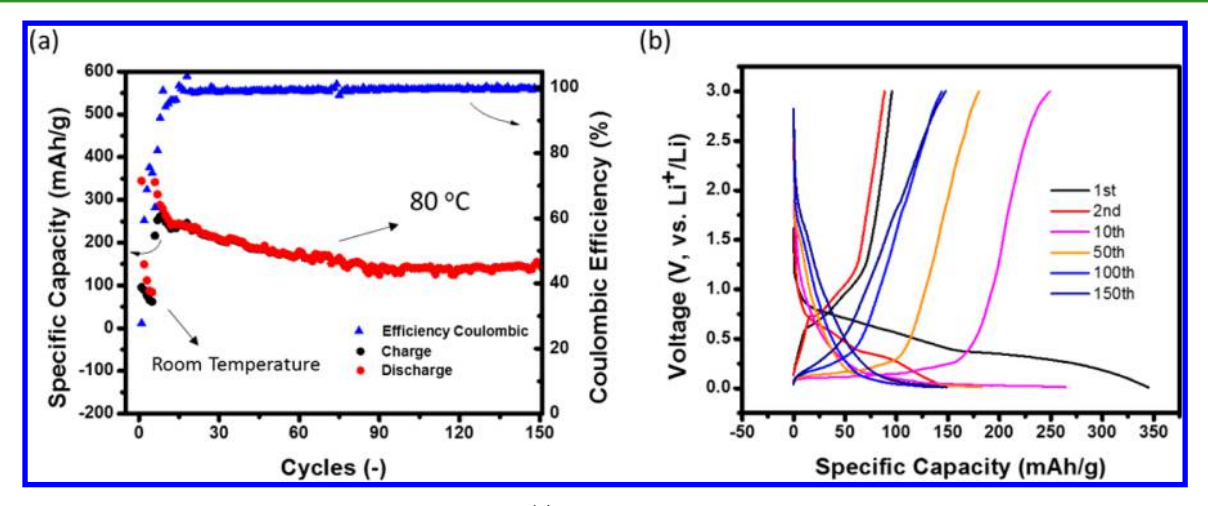


Figure 11. Cycling performance and Coulombic efficiencies with (a) sPS ionogel membrane at 80 °C, activated with five cycles at room temperature and (b) corresponding charge/discharge profiles.

shown for the cells with sPS and the Celgard-3501 ionogel membranes at 25 and 100 °C. It is seen that the bulk resistances and the charge transfer resistances are larger for Celgard-3501 ionogel membranes in comparison to sPS ionogel membranes. This is in agreement with the ionic conductivity data reported in Table 3. At 25 °C, the Celgard-3501 ionogel membrane has higher bulk resistance  $(R_b)$  of approximately 34  $\Omega$ , whereas the sPS ionogel membrane has a  $R_b$  value of 17  $\Omega$ , attributed to better compatibility of the ionic liquid electrolyte with sPS strands in the membrane. At 100 °C, the sPS ionogel membrane also exhibited lower values of R<sub>b</sub> and charge transfer resistance  $(R_{ct})$ , indicating better performance of the sPS ionogel membrane than Celgard-3501 ionogel membrane. The lower  $R_{ct}$  value is the result of higher electrolyte retention for sPS ionogel membrane (Table 3) and higher wettability of sPS strands by the IL as seen from the contact angle data.<sup>32</sup> Obviously, the low R<sub>ct</sub> value indicates that sPS ionogel membrane helps improve the connection between the anode and the cathode, thus providing better interfacial contact at the electrodes.

To measure the electrochemical stability of cells fabricated with Celgard-3501 ionogel and sPS ionogel membranes, linear sweep voltammetry (LSV) was conducted in the voltage range of 0 to 7 V (vs. Li<sup>+</sup>/Li, Figure 9). As it can be seen from the LSV data, the cell with sPS ionogel membranes exhibited much better electrochemical stability than with Celgard-3501 ionogel membranes. At room temperature, sPS ionogel membranes exhibited better electrochemical stability in comparison to Celgard-3501 ionogel membrane as can be seen from the data presented in Figure 9a and b. The dotted lines in Figure 9 indicate the failure of the sPS membrane at approximately 5.2 V, whereas the solid line indicates the initiation of membrane deterioration at 4.8 V. The cell fabricated with Celgard-3501 ionogel membrane had a voltage stability only up to 4.8 V, which is 0.4 V lower than the cell fabricated with sPS ionogel membrane. At 100 °C, the cell fabricated from sPS ionogel membrane exhibited good electrochemical stability up to 4.8 V (see Figure 9c), while the cell containing Celgard-3501 ionogel membrane failed in the LSV test, due to deterioration and shrinkage of the Celgard-3501 ionogel membrane as discussed previously.

To demonstrate the cycle stability of sPS ionogel membrane for rechargeable Li-ion batteries, Li/sPS-IL/graphite cells were fabricated and tested at room temperature, under a current rate of 100 mA/g in the voltage range from 0.005-3 V. For comparison, Li/sPS-IL/graphite cells were also assembled and tested under the same condition. In Figure 10a and b, the galvanostatic charge and discharge of the cells fabricated with Celgard-3501 and sPS ionogel membranes are shown. The cell with sPS ionogel membranes rendered better reversible specific capacity of 70 mAh/g at room temperature compared to 30 mAh/g for the cell containing Celgard-3501 ionogel membrane. Both the initial cycles exhibited specific capacity fading, which can be attributed to the formation of the SEI layer. However, as the half-cell stabilizes, the capacity for the sPS-IL reaches higher reversible value with Coulombic efficiency around ~97% in the following cycles. Better performance of cells with sPS ionogel membranes is attributed to lower charge transfer resistance  $(R_{ct})$  and higher ionic conductivity of sPS ionogel system. 33,34

To explore the cell performance at high temperature, rate capability test of Li/sPS ionogel/graphite cells was done at 80 °C (as shown in Figure S1). The test was conducted at different rates (100 mA/g, 200 mA/g, 500 mA/g, and 2 A/g) from 0.01–3.00 V. The battery exhibited a specific capacity of 410 mAh/g, 393 mAh/g, 143 mAh/g, and 82 mAh/g, respectively. It can be observed that, even with high rate 2 A/g at 80 °C, the cell could reach relatively good specific capacity. This good rate performance was due to high ionic conductivity and low interfacial resistance of sPS ionogel as well. Therefore, the sPS ionogel showed great rate capability at high temperature.

To further confirm the superior cycle stability at high temperature, long cycle performance tests of both Li/sPS ionogel/graphite and Li/Celgard-3501 ionogel/graphite cells were conducted. Because of poor thermal stability (as seen in Figure 5), cells with Celgard-3501 membrane were not able to run at such high temperature and always failed after the first few cycles, caused by shrinkage of the membrane, which finally led to internal short circuit. The cells with sPS ionogel membrane (Figure 11) could still render capacity around 160 mAh/g (at 100 mA/g) and 52% capacity retention on their 150th cycle with 96.4% average Coulombic efficiency, indicating sPS membrane was thermally as well as electrochemically stable enough to perform at high temperature, which is beneficial for safety concern in LIB. At higher operating temperatures, growth rate of solid electrolyte layer (SEI) was higher and also the formation of graphite intercalation compounds (GIC) was enhanced.35,36 In view of this, the long cycle tests were performed at 80 °C, instead of 100 °C, to observe the long-term performance of the cell. On the basis of the above discussions, it can be concluded that the sPS ionogel membrane is an excellent and suitable substitute membrane compared to Celgard-3501 ionogel membrane for both low and high temperature LIB applications. Two recent studies<sup>37,38</sup> reported a set of inorganic—organic hybrid ionogel materials also with high thermal stability and excellent high temperature Li-ion battery performance.

### CONCLUSIONS

This paper reported a simple two-step procedure for fabrication of sPS ionogel membrane, which was found to be stable for high temperature electrochemical operation, such in LIBs. The porosity of sPS ionogel membranes was significantly higher than that of Celgard-3501 ionogel membranes, which accounted for high IL to polymer weight ratio in the membranes and produced high room temperature conductivity of  $6.33 \times 10^{-4}$  S/cm. The contact angle data showed better wettability of sPS membrane with IL and EC/DEC electrolytes. The high porosity and better wettability of sPS by the electrolyte resulted in lower impedance for sPS ionogels compared to Celgard-3501 ionogel membranes at 25 and 100 °C. The impedance spectroscopy data indicated low bulk charge transfer resistance of sPS-ionogel attributed to better wettability and electrolyte retention of sPS-IL system. The LSV data show improved performance for sPS ionogel membrane over Celgard ionogel membrane at 25 °C. The sPS ionogel membrane also indicated stable electrochemical window up to 4.8 V at 100 °C. This electrochemical and thermal stability of sPS-ionogel allowed continuous operation of LIB cell at 100 °C.

#### ASSOCIATED CONTENT

# S Supporting Information

The Supporting Information is available free of charge on the ACS Publications website at DOI: 10.1021/acsami.7b09155.

Additional data on rate capacity test (PDF)

# AUTHOR INFORMATION

# **Corresponding Author**

\*E-mail: janas@uakron.edu.

ORCID ®

Sadhan C. Jana: 0000-0001-8962-380X

Notes

The authors declare no competing financial interest.

### ACKNOWLEDGMENTS

The authors would like to thank Yunfan Shao, E. Laughlin, and K. Jackson of The University of Akron. W.L., Y.C., and Y.Z. thank the support from National Science Foundation (NSF) through NSF-CBET 1505943 and ACS Petroleum Research Fund (PRF# 53560 -DNI 10).

#### REFERENCES

- (1) Li, Q.; Liu, F.; Yang, T.; Gadinski, M. R.; Zhang, G.; Chen, L.-Q.; Wang, Q. Sandwich-Structured Polymer Nanocomposites with High Energy Density and Great Charge—discharge Efficiency at Elevated Temperatures. *Proc. Natl. Acad. Sci. U. S. A.* **2016**, *113* (36), 9995—10000
- (2) Armand, M.; Tarascon, J.-M. Building Better Batteries. *Nature* **2008**, *451* (7179), *652*–*657*.

- (3) Wen, J.; Yu, Y.; Chen, C. A Review on Lithium-Ion Batteries Safety Issues: Existing Problems and Possible Solutions. *Mater. Express* **2012**, 2 (3), 197–212.
- (4) Plylahan, N.; Kerner, M.; Lim, D. H.; Matic, A.; Johansson, P. Ionic Liquid and Hybrid Ionic Liquid/organic Electrolytes for High Temperature Lithium-Ion Battery Application. *Electrochim. Acta* **2016**, 216, 24–34.
- (5) Smith, B. DOT HS 811 573; NHTSA, Office of Vehicle Safety Compliance, 2012.
- (6) Bandhauer, T. M.; Garimella, S.; Fuller, T. F. A Critical Review of Thermal Issues in Lithium-Ion Batteries. *J. Electrochem. Soc.* **2011**, *158* (3), R1–R25.
- (7) Sato, T.; Maruo, T.; Marukane, S.; Takagi, K. Ionic Liquids Containing Carbonate Solvent as Electrolytes for Lithium Ion Cells. *J. Power Sources* **2004**, *138* (1–2), 253–261.
- (8) Paillard, E.; Zhou, Q.; Henderson, W. A.; Appetecchi, G. B.; Montanino, M.; Passerini, S. Electrochemical and Physicochemical Properties of PY 14 FSI-Based Electrolytes with LiFSI. *J. Electrochem. Soc.* 2009, 156 (11), 891–895.
- (9) Wang, Q.; Ping, P.; Zhao, X.; Chu, G.; Sun, J.; Chen, C. Thermal Runaway Caused Fire and Explosion of Lithium Ion Battery. *J. Power Sources* **2012**, 208, 210–224.
- (10) Samsung Electronics Cites Assembly, Manufacturing Defects in Note 7 Battery Fires; CNBC, 2017. http://www.cnbc.com/2017/01/22/samsung-news-galaxy-note-7-fires-caused-by-irregular-batteries.html (accessed Mar 8, 2017).
- (11) Samsung Electronics Announces Cause of Galaxy Note7 Incidents in Press Conference; Samsung Newsroom, 2017. https://news.samsung.com/global/samsung-electronics-announces-cause-of-galaxy-note7-incidents-in-press-conference (accessed Mar 8, 2017).
- (12) Armand, M.; Endres, F.; MacFarlane, D. R.; Ohno, H.; Scrosati, B. Ionic-Liquid Materials for the Electrochemical Challenges of the Future. *Nat. Mater.* **2009**, *8* (8), 621–629.
- (13) Lewandowski, A.; Swiderska-Mocek, A. Ionic Liquids as Electrolytes for Li-Ion Batteries An Overview of Electrochemical Studies. *J. Power Sources* **2009**, 194 (2), 601–609.
- (14) Martinelli, A.; Matic, A.; Jacobsson, P.; Borjesson, L.; Fernicola, A.; Scrosati, B. Phase Behavior and Ionic Conductivity in Lithium Bis (Trifluoromethanesulfonyl) Imide-Doped Ionic Liquids of the Pyrrolidinium Cation and Bis (Trifluoromethanesulfonyl) Imide Anion. J. Phys. Chem. B 2009, 113 (32), 11247–11251.
- (15) Henderson, W.; Passerini, S. Phase Behavior of Ionic Liquid LiX Mixtures: Pyrrolidinium Cations and TFSI- Anions. *Chem. Mater.* **2004**, *16* (15), 2881–2885.
- (16) Di Leo, R. A.; Marschilok, A. C.; Takeuchi, K. J.; Takeuchi, E. S. Battery Electrolytes Based on Saturated Ring Ionic Liquids: Physical and Electrochemical Properties. *Electrochim. Acta* **2013**, *109*, 27–32.
- (17) Ong, S. P.; Andreussi, O.; Wu, Y.; Marzari, N.; Ceder, G. Electrochemical Windows of Room-Temperature Ionic Liquids from Molecular Dynamics and Density Functional Theory Calculations. *Chem. Mater.* **2011**, 23 (11), 2979–2986.
- (18) Le Bideau, J.; Viau, L.; Vioux, A. Ionogels, Ionic Liquid Based Hybrid Materials. *Chem. Soc. Rev.* **2011**, *40* (2), 907–925.
- (19) Neouze, M.; Le Bideau, J.; Gaveau, P.; Bellayer, S.; Vioux, A. Ionogels, New Materials Arising from the Confinement of Ionic Liquids within Silica-Derived Networks. *Chem. Mater.* **2006**, *18* (17), 3931–3936.
- (20) Le Bideau, J.; Gaveau, P.; Bellayer, S.; Néouze, M.; Vioux, A. Effect of Confinement on Ionic Liquids Dynamics in Monolithic Silica Ionogels: 1H NMR Study. *Phys. Chem. Chem. Phys.* **2007**, *9*, 5419–5422.
- (21) Chen, S.; Wu, G.; Sha, M.; Huang, S. Transition of Ionic Liquid [Bmim] [PF6] from Liquid to High-Melting-Point Crystal When Confined in Multiwalled Carbon Nanotubes. *J. Am. Chem. Soc.* **2007**, 129 (9), 2416–2417.
- (22) Wang, X.; Jana, S. C. Tailoring of Morphology and Surface Properties of Syndiotactic Polystyrene Aerogels. *Langmuir* **2013**, *29*, 5589–5598.

- (23) Daniel, C.; Dammer, C.; Guenet, J. On the Definition of Thermoreversible Gels: The Case of Syndiotactic Polystyrene. *Polymer* **1994**, 35 (19), 4243–4246.
- (24) Arora, P.; Zhang, Z. Battery Separators. Chem. Rev. 2004, 104 (10), 4419–4462.
- (25) Meador, M. A. B.; Cubon, V. A.; Scheiman, D.; Bennett, W. R. Effect of Branching on Rod-coil Block Polyimides as Membrane Materials for Lithium Polymer Batteries. *Chem. Mater.* **2003**, *15*, 3018–3025.
- (26) Tigelaar, D. M.; Palker, A. E.; Meador, M. A. B.; Bennett, W. R. Synthesis and compatibility of Ionic Liquid Containing Rod-Coil Polyimide Gel Electrolytes with Lithium Metal Electrodes. *J. Electrochem. Soc.* **2008**, *155*, A768–A774.
- (27) MacMullin, R. B.; Muccini, G. A. Characteristics of Porous Beds and Structures. *AIChE J.* **1956**, 2 (3), 393–403.
- (28) Vranes, M.; Dozic, S.; Djeric, V.; Gadzuric, S. Physicochemical Characterization of 1-Butyl-3-Methylimidazolium and 1-Butyl-1-Methylpyrrolidinium Bis(trifluoromethylsulfonyl)imide. *J. Chem. Eng. Data* **2012**, *57* (4), 1072–1077.
- (29) Hasegawa, Y.; Takihana, J.; Ohki, Y. Estimation Of Thermal Expansion Coefficients Of Polymeric Insulating Films From Temperature Dependence Of Dielectric Permittivity. *Jpn. J. Appl. Phys.* **2014**, *53* (7), 071501–4.
- (30) Rizzo, P.; Albunia, A. R.; Guerra, G. Syndiotactic Polystyrene Films with Different Uniplanar Orientations: Additional Information on Crystal Phase Transitions. *Macromol. Chem. Phys.* **2013**, 214, 41–45.
- (31) Martinez-Cisneros, C.; Antonelli, C.; Levenfeld, B.; Varez, A.; Sanchez, J. Y. Evaluation of Polyolefin-Based Macroporous Separators for High Temperature Li-Ion Batteries. *Electrochim. Acta* **2016**, 216, 68–78.
- (32) Chun, S.-J.; Choi, E.-S.; Lee, E.-H.; Kim, J. H.; Lee, S.-Y. S.-Y.; Lee, S.-Y. S.-Y. Eco-Friendly Cellulose Nanofiber Paper-Derived Separator Membranes Featuring Tunable Nanoporous Network Channels for Lithium-Ion Batteries. *J. Mater. Chem.* **2012**, 22 (32), 16618.
- (33) Kim, J. Y.; Lim, D. Y. Surface-Modified Membrane as a Separator for Lithium-Ion Polymer Battery. *Energies* **2010**, 3 (4), 866–885
- (34) Prasanth, R.; Aravindan, V.; Srinivasan, M. Novel Polymer Electrolyte Based on Cob-Web Electrospun Multi Component Polymer Blend of Polyacrylonitrile/poly(methyl Methacrylate)/polystyrene for Lithium Ion Batteries Preparation and Electrochemical Characterization. *J. Power Sources* **2012**, 202, 299–307.
- (35) Waldmann, T.; Wilka, M.; Kasper, M.; Fleischhammer, M.; Wohlfahrt-Mehrens, M. Temperature Dependent Ageing Mechanisms in Lithium-ion Batteries: A Post-Mortem Study. *J. Power Sources* **2014**, 262, 129–135.
- (36) Leng, F.; Tan, C. M.; Pecht, M. Effect of Temperature on the Aging rate of Li Ion Battery Operating above Room Temperature. *Sci. Rep.* **2015**, *5*, 12967.
- (37) Lee, J. H.; Lee, A. S.; Lee, J.-C.; Hong, S. M.; Hwang, S. S.; Koo, C. M. Hybrid Ionogel Electrolytes For High Temperature Lithium Batteries. *J. Mater. Chem. A* **2015**, *3*, 2226–2233.
- (38) Na, W.; Lee, A. S.; Lee, J. H.; Hwang, S. S.; Hong, S. M.; Kim, E.; Koo, C. M. Lithium Ion Capacitors Fabricated With Polyethylene Oxide-functionalized Polysilsesquioxane Hybrid Ionogel Electrolytes. *Electrochim. Acta* **2016**, *188*, 582–588.